

# A PARAMETERIZATION WITH WAVE SATURATION ADJUSTMENT OF SUBGRID-SCALE AVERAGE WAVE STRESS OVER THREE-DIMENSIONAL TOPOGRAPHY

Carmen J. Nappo\*

*CJN Research Meteorology, Knoxville, TN 37919 U.S.A.*

Gunilla Svensson

Department of Meteorology, Stockholm University, Stockholm, Sweden

## 1. Introduction.

Nappo and Chimonas (1992) demonstrated that internal gravity waves launched by small-scale topography could be as important in the planetary boundary layer as the large-scale mountain waves are in the free atmosphere. Steeneveld *et al* (2008a, b) have used a high-resolution version of the MM5 model to show that wave drag over the gentle terrain of the CASES-99 field site (Poulos *et al.*, 2002) can be important in large-scale processes and possibly account for under estimated turbulence in mesoscale models. Tjernström *et al.* (2008) observed intermittent fine-scale turbulence structures in the nocturnal residual layer during one night of the CASES-99 experiment but not on another night. Using a three-dimensional linear gravity wave model and observed meteorological profiles, they showed that the calculated wave stress divergence was large in the residual layer during the turbulence night, but near zero in the residual layer during the calm night.

In this extended abstract, we describe the linear gravity wave model used in Tjernström *et al.* (2008), and present an example of its application to a region of the eastern Tennessee River Valley, a region we consider to be of moderate relief. What makes this model unique is a parameterization of wave breaking, which is a non-linear process.

## 2. The model.

Parameterizations of wave stress divergence in GCMs and large-scale forecast models are routinely used (see, for example, Baines, 1995; Nappo, 2002 and references therein). Bretherton (1969), Hines (1988), and Shutts (1995) calculated

wave stress over three-dimensional terrains. It is important to note that these parameterizations and model studies used the WKB method (Baines, 1995; Bender and Orzag 1999; Nappo 2002). Under this method, the mean wind and stratification varies on a vertical scale greater than the vertical wavelength so that the wave appears to be propagating in a quasi-uniform medium. Because of this assumption, wave reflections cannot occur, *i.e.*, all the waves are upward propagating.

When calculating gravity waves over three-dimensional topography, each horizontal projection of the surface wind,  $U_\phi(0)$ , will pass over terrain features that will launch gravity waves. Here,

$$U_\phi(0) = U(0)\cos[\phi - \beta(0)] \quad (1)$$

where  $U(0)$  is the surface wind with bearing (direction toward)  $\beta(0)$ , and  $\beta(z)$  is the vertical profile of the mean wind direction. Each horizontal projection defines a wave vector. This wave vector lies in the  $\phi - \beta(0)$  direction and is a function of the wind profile in that direction. The total wave field is the sum of the waves generated by each of these projections. Accordingly, the wave perturbations must be calculated for all wind components within  $\pm \pi/2$  of  $\beta(0)$ .

When the background wind turns with height, there will be a level where the wind vector is normal to some wave vector. When this happens, the background wind speed for that wave vector is zero, and a critical level exists for that wave. Wave dissipation occurs at a critical level. For example, if the Richardson number at a critical level equals 1, then the wave stress is reduced by a factor 0.004 (see, for example, Baines, 1995;

---

\*Corresponding author: 907 Heather Way,  
Knoxville, TN 37919, cjn\_met@comcast.net.

Nappo, 2002). Thus, for practical purposes we can assume complete wave dissipation at a critical level. Above the critical level, that wave will no longer contribute to the wave field. Shutts (1995) gives a detailed account and some examples of this process. A direct consequence of critical levels is a turning of the wave stress with height such that average wave stress is not opposite to the mean wind.

The wave stresses  $\tau_x$  and  $\tau_y$  are calculated in the directions  $\phi$  within the sector  $\beta(0) - \pi/2 \leq \phi(z) \leq \beta(0) + \pi/2$ . For each direction, the Taylor-Goldstein equation takes the two-dimensional form:

$$\frac{d^2}{dz^2} \widehat{w}_\phi(\kappa, z) + \left[ \frac{N^2}{U_\phi^2} - \frac{U_\phi''}{U_\phi} - \kappa^2 \right] \widehat{w}_\phi(\kappa, z) = 0 \quad (2)$$

where  $\widehat{w}_\phi$  is the Fourier-transform of the vertical velocity perturbation,  $N$  is the Brunt-Väisälä frequency, the primes denote the vertical derivative, and  $\kappa$  is the horizontal wavenumber in the  $\phi$ -direction. The background winds  $U_\phi(z)$  are given by (1). At the top of the wave model we impose the radiation condition, and at the bottom the boundary condition is:

$$\widehat{w}_\phi(0) = i\kappa u_\phi(0) \widehat{h}_\phi(\kappa) \quad (3)$$

where  $\widehat{h}_\phi(\kappa)$  is the Fourier transform of the terrain height along the  $\phi$ -direction. The horizontal wave perturbation velocity is given by:

$$\widehat{u}_\phi = \frac{i}{\kappa} \frac{\partial \widehat{w}_\phi}{\partial z} \quad (4)$$

where  $i = \sqrt{-1}$ . The wave perturbation velocities in physical space,  $u_\phi(\ell, z)$  and  $w_\phi(\ell, z)$ , are given by the inverse Fourier transforms of  $\widehat{u}_\phi(\kappa, z)$  and  $\widehat{w}_\phi(\kappa, z)$  respectively, where  $\ell$  is the horizontal distance in the  $\phi$ -direction.

As mentioned above, most calculations of wave stress used the WKB method (see, for example, Grisogono, 1994). However, in the stable PBL the vertical variation of the mean wind speed and stratification changes on a vertical scale that is generally less than the vertical wavelengths of the dominant waves. To scale the problem, consider a wave generated by an obstacle of scale width  $b$  in a constant stratified flow. The most energetic wave will have wavenumber  $\kappa = 1/b$ . In the linear wave theory, the vertical wavelength of this wave is:

$$\lambda_z = 2\pi / m = 2\pi \left( \frac{N^2}{U^2} - \frac{1}{b^2} \right)^{-\frac{1}{2}} \quad (5)$$

where  $m$  is the vertical wavenumber. Now let  $b = 1000$  m, then for typical boundary layer values of  $U = 5$  ms<sup>-1</sup> and  $N = 0.03$  s<sup>-1</sup>,  $\lambda_z = 1060$  m. A reasonable scale for the vertical variation of the boundary-layer flow is the Ekman-layer depth,  $z_E = \pi \sqrt{2k/f}$  where  $k$  is the eddy coefficient for friction, and  $f$  is the Coriolis parameter. Using a value  $\kappa = 2$  m<sup>2</sup> s<sup>-1</sup> and  $f = 10^{-4}$  s<sup>-1</sup>,  $z_E = 630$  m. We see that the vertical wavelength is greater than the vertical variation of the background quantities, and wave reflections can occur. Thus, in the stable PBL the WKB method may not be applicable. Accordingly, the full Taylor-Goldstein equation (2) must be solve.

## 2.2 Wave breaking parameterization.

Bretherton (1969) and Shutts (1995) considered only wave dissipation at critical levels. However, as a wave approaches a critical level its amplitude increases and eventually becomes convectively unstable and breaks (see, for example, Booker and Bretherton, 1967; Fritts, 1984; Nappo, 2002). Hence, wave dissipation can begin before the critical level is reached. However, these non-linear effects are not in the linear theory and must be parameterized. An often-used parameterization requires that the total flow is convectively stable everywhere, *i.e.*

$$\frac{\partial}{\partial z} (\theta_0 + \theta_1) > 0, \quad (6)$$

where  $\theta_0$  and  $\theta_1$  are the background and wave-perturbation potential temperatures respectively. In order to maintain condition (6), the amplitudes of the upwelling gravity waves are reduced as needed. While this is straightforward in the WKB method where only upward propagating waves are allowed, such a method is problematical in the PBL because both upward and downward (reflected) propagating waves can occur. As an alternative parameterization, Dörnbrack and Nappo (1997), Nappo and Physick (1998), and Nappo *et al* (2004) demonstrated that a convectively stable wave field can be maintained by systematically lowering the heights of the underlying terrain.

In this ‘terrain-height adjustment’ scheme, it is required that:

$$\left| \frac{u_\phi}{U} \right| < 1 \quad (7)$$

*i.e.*, flow blocking is not allowed. Note that convective instability and flow blocking occur simultaneously. After  $u_\phi(\ell, z)$  is calculated, condition (7) is tested using the maximum value of  $u_\phi$  at each model level beginning at the ground surface. If (7) fails,  $\hat{h}_\phi(\kappa)$  is reduced by 5%, and  $\hat{w}_\phi$  and  $\hat{u}_\phi$  are and their inverse transforms,  $u_\phi$  and  $w_\phi$  are re-calculated. Test (7) is repeated, and if not satisfied,  $\hat{h}_\phi(\kappa)$  is reduced another 5%, *etc.* When (7) is satisfied, the testing process proceeds to the next higher level of the wave model, but now  $\hat{h}_\phi(\kappa)$  has the final values from the previous adjustment at the lower level. This process continues, and if a level is reached where  $\hat{h}_\phi(\kappa)$  becomes very small, we assume the waves have been completely dissipated. If a critical level exists, then wave amplitudes are decreased linearly from the breaking level to the critical level.

### 2.3 Wave stress

After all the values of  $u_\phi(\ell, z)$  and  $w_\phi(\ell, z)$  have been adjusted so that convectively unstable regions are absent, the area-averaged wave stresses are calculated using:

$$\bar{\tau}_x(z) = \frac{1}{XY} \sum_{j=1}^M \tau_{x,\phi_j}(z) \quad (8)$$

$$\bar{\tau}_y(z) = \frac{1}{XY} \sum_{j=1}^M \tau_{y,\phi_j}(z) \quad (9)$$

where

$$\tau_{x,\phi_j}(z) = -\rho_0 \int_{-\frac{L}{2}}^{\frac{L}{2}} u_{\phi_j}(\ell, z) w_{\phi_j}(\ell, z) \sin \phi_j d\ell \quad (10)$$

and

$$\tau_{y,\phi_j}(z) = -\rho_0 \int_{-\frac{L}{2}}^{\frac{L}{2}} u_{\phi_j}(\ell, z) w_{\phi_j}(\ell, z) \cos \phi_j d\ell \quad (11)$$

where  $\rho_0$  is the atmospheric density,  $M$  is the number azimuth angles along which the stresses are calculated,  $X$  and  $Y$  are the dimensions of the domain and  $L^2 = X^2 + Y^2$ .

### 3. Results

As an example, we apply the parameterization to the topography of the eastern portion of the Tennessee River Valley, near Knoxville, TN. Figure 1 shows a contour map of the region. Counter heights are

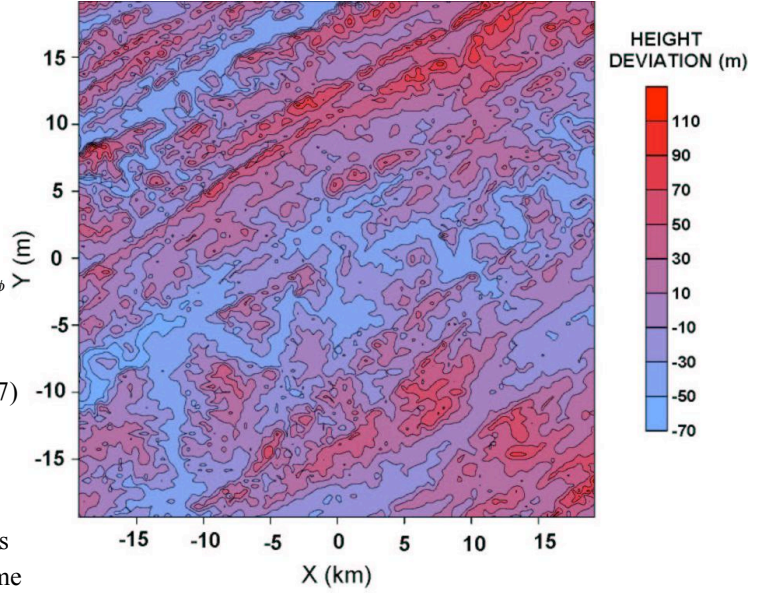


Figure 1 Eastern Tennessee River Valley topography; contours are relative to the area mean height of 280 M MSL.

relative to an area-mean average height of about 289 m MSL. The terrain grid consists of  $321 \times 321$  points with a spacing of 120 m. The domain size is about  $38 \times 38$  km. The nearly parallel ridges extending from SW to NE are a characteristic feature of the valley. The ridges are typically about 100 m high, 1000 m wide, and separated by about 1 to 2 km. For this domain, the rms value of the terrain height is about 28 m.

Figure 2 shows tethersonde profiles of wind speed, wind direction, and Brunt-Väisälä frequency taken near Oak Ridge, TN on 19 July 1987 at about 8:37 EDT. The winds were moderate, and from the east to northeast. From the ground surface up to about 200 m, the wind backed from about  $85^\circ$  to about  $45^\circ$ . Above 200 m, the winds veered toward the east. In our model calculations, wind speed, wind direction, and potential temperature were held constant below 40 m. For these calculations,  $X=Y=L=38,000$  m, The angular domain,  $\phi$ , was divided into 36 10-degree sectors. The wave model extended up to 600 m.

Figure 3 shows the calculated profiles of  $\bar{\tau}_x$  and  $\bar{\tau}_y$  with and without 'adjustment' for wave breaking. Below about 40 m, there is not a great difference between the two methods. At the ground surface,  $\bar{\tau}$  is about  $7.8 \times 10^{-5}$  Pa toward  $139^\circ$  without adjustment, and about  $6.8 \times 10^{-5}$  Pa toward  $140^\circ$  with adjustment. Between the ground surface and about 100 m, the unadjusted waves show a nearly uniform stress with height, but the adjusted wave stress shows a near-continuous decrease with height, especially for  $\bar{\tau}_y$ . Between about 100 and 200 m, the unadjusted wave stress decreases

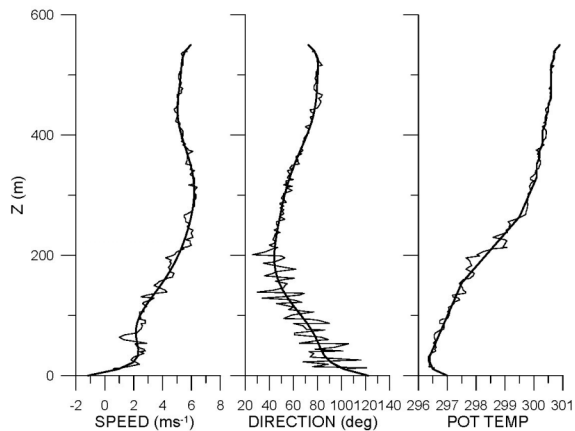


Figure 2 Speed, direction, and potential temp profiles; heavy lines denote polynomial fits used in the calculations.

markedly with height. This decrease is due to wave absorption at critical levels. From Figure 2, the wind direction between these heights backs about  $40^\circ$ , and this wind shear is the source of the critical levels. Above 200 m, the adjusted and unadjusted stresses become nearly constant with height. This is especially the case for the adjusted wave stress. However, from Figure 2 we see that wind direction continues to veer, and thus critical levels must be present in this region, and we would expect further wave dissipation. This question will be discussed in the next Section.

We can compare the wave stress at the ground surface with the friction stress by assuming a drag coefficient of 0.0014 (Stull, 1988) and a surface wind speed of  $1.4 \text{ ms}^{-1}$ , which is the average observed wind speed between the near-ground surface and 40 m. This gives a value of  $137 \times 10^{-5} \text{ Pa}$ , which is about 17 times greater than the wave stress. Also, the friction stress acts toward about  $100^\circ$ , which is the average observed wind direction between the near-ground surface and 40 m.

#### 4. Discussion

The profiles of wave stress shown in Figure 3 illustrate the effects of including wave breaking.

##### 4.1 Without wave breaking

For the stress profiles calculated without wave breaking, wave dissipation results only from wave absorption at critical levels. However, at some heights the average wave stress increases with height. At first sight, this is unexpected since we

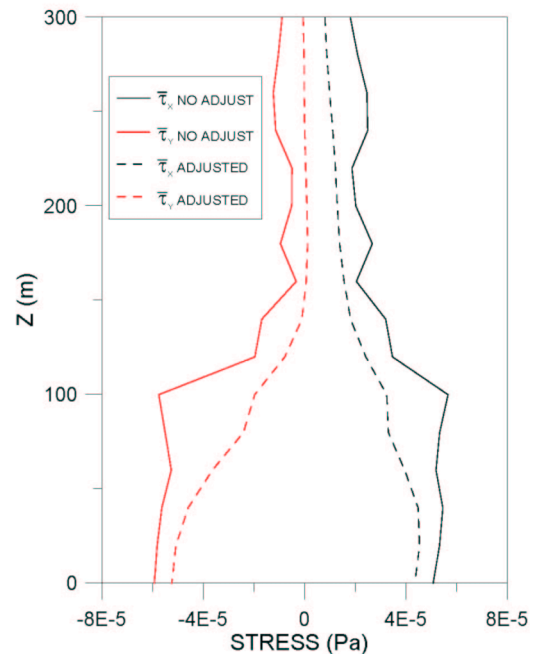


Figure 3 Area-averaged wave stress over region shown in Fig. 1 calculated with and without wave-breaking parameterization.

are accustomed to thinking that wave stress must be either constant or decreasing with height. The wave stress in a given direction is a function of the terrain-height and wind speed profile in that direction. In some directions at some heights, the wave stress may be greater than those in other directions at lower heights. This will result in an increase of the area-averaged stress. Above about 200 m, the average wave stress is relatively constant; however, wind-direction shear exists in this region (Fig. 2), and we expect critical levels and wave dissipation there. However, although wind turning causes critical levels, these critical levels need not exist for all wind directions. Accordingly, there will be some directions where the wave stress will be constant with height

If the wave stresses calculated without breaking were used in a numerical model, then regions of stress convergence rather than divergence are possible. This would lead to an acceleration of the model flow, which is physically unreasonable.

##### 4.2 With wave breaking

When the wave-breaking parameterization is included, a much different stress profile is calculated. Now the wave stress decreases almost uniformly and smoothly with height. Above 150 m, the wave stresses are almost constant, which is in contrast with the non-breaking case where the average wave stresses increase at some heights. As

mentioned above, critical levels will not exist for some directions; however, because of wave breaking, there are no levels of increasing wave stress.

## 5. Conclusions

We have applied a linear gravity model that includes a parameterization of non-linear wave breaking to a region of the eastern Tennessee River Valley near Knoxville, Tennessee. We have also used real profiles of wind speed, wind direction and potential temperature. The resulting area-averaged wave stress profiles are smooth and continuously decreasing in value. The maximum wave stress near the ground surface is about a factor 20 less than the estimated friction stress. The direction of the wave stress at the ground surface differs from the direction of the friction stress by about 40°. Although the wave stresses are small relative to the friction stress, the momentum deposited above the ground surface may have significant effects in a time-dependent numerical model.

## Acknowledgements

This work was funded by the International Meteorological Institute, when the first author was a visiting scientist at the Department of Meteorology, Stockholm University. Special thanks to Thorsten Mauritsen, Gert-Jan Steeneveld, and Branko Grisogono for their suggestions and comments.

## References

- Baines, P. G., 1995: *Topographic Effects in Stratified flows*. New York: Cambridge Univ. Press.
- Bender, C. M. and S. A. Orzag, 1999: *Advanced Mathematical Methods for Scientists and Engineers*, Springer-Verlag, New York, pp 593.
- Booker, J. R. and Bretherton, F. P., 1967: The critical level for internal gravity waves in a shear flow. *J. Fluid Mech.*, **27**, 513-539.
- Bretherton, F. P., 1969: Momentum transport by gravity waves. *Quart. J. R. Met. Soc.*, **95**, 213-243.
- Dörnbrack, A. and C. J. Nappo, 1997: A note on the application of linear wave theory at a critical level. *Boundary-Layer Meteorology*, **82**: 399-416.
- Fritts, D. C., 1984: Gravity wave saturation in the middle atmosphere. A review of theory and observations. *Rev. Geophys. Space Phys.*, **22**, 275-308.
- Grisogono, B., 1994: Dissipation of waves in the atmospheric boundary layer. *J. Atmos. Sci.*, **51**, 1237-1243.
- Hines, C. O., 1988: A modeling of atmospheric gravity waves and wave drag generated by isotropic and anisotropic terrain, *J. Atmos. Sci.*, **45**, 309-322.
- Nappo, C. J. and G. Chimonas, 1992: Wave exchange between the ground surface and a boundary layer critical level. *Journal of Atmospheric Science* **49**:1075-1091.
- Nappo C. J. and W. Physick, 1998: Gravity Wave Stress Parameterization In A Mesoscale Model. In: *Air Pollution Modeling and Its Applications X*, NATO Challenges of Modern Society, Vol. 23. Edited by Sven-Erik Gryning and F. A. Schiermeier, Plenum Press, NewYork.
- Nappo, C. J., 2002: *An Introduction to Atmospheric Gravity Waves.*, Academic Press, pp 260.
- Nappo, C. J., H-Y Chun, and H-J Lee, 2004: A parameterization of terrain-induced gravity wave stress in boundary-layer models. *Atmospheric Environment*, **38**, 2665-2675
- Poulos, G.S., and co-authors, 2002: CASES-99: A comprehensive Investigation of the stable nocturnal boundary layer, *Bull. Amer. Meteor. Soc.*, **83**, 555-581
- Shutts, G., 1995: Gravity-wave drag parameterization over complex terrain: The effects of critical-level absorption in directional wind-shear, *Quart. J. R. Met. Soc.*, **121**, 1005-1021.
- Steeneveld, G. J., C. J. Nappo, and A. A. M. Holtslag, 2008a: Further examination of the possible role of orographically induced wave drag in the stable boundary layer during CASES99. *Am. Meteorol. Soc.* 18'th Symposium on Boundary Layers and Turbulence, 9-13 June 2008, Stockholm, Sweden
- Steeneveld, G.J., A.A.M. Holtslag, C.J. Nappo, B.J.H. van de Wiel, and L. Mahrt, 2008b: Exploring the possible role of small scale terrain drag on stable boundary layers over land. To appear in *J. Appl. Meteorol. Climatology*.
- Tjernström, M., B.B. Balsley, G. Svensson, and C.J. Nappo, 2008: The effects of critical layers on residual layer turbulence. To appear in *J. Atmos. Sci.*